

Advance Publication by J-STAGE

Mechanical Engineering Journal

DOI: 10.1299/mej.22-00028

Received date : 16 January, 2022

Accepted date : 27 April, 2022

J-STAGE Advance Publication date : 11 May, 2022



© 2022 The Japan Society of Mechanical Engineers. This is an open access article under the terms of the Creative Commons Attribution-NonCommercial-NoDerivs license (<https://creativecommons.org/licenses/by-nc-nd/4.0/>).

Cost estimation of CCS integration into thermal power plants in Japan

Hirotaka ISOGAI*, Corey Adam MYERS* and Takao NAKAGAKI*

*Waseda University

3-4-1 Okubo, Shinjuku-ku, Tokyo 169-8555, Japan

E-mail: spi_tz@asagi.waseda.jp

Abstract

Carbon capture and storage (CCS) is an important technology to reduce CO₂ emissions from power and industry. To accelerate large-scale CCS deployment, further reduction of the cost to implement the full technology chain is necessary. Full chain CCS cost depends on multiple technological, market, and societal factors. Therefore, case-specific cost analysis is important. This study estimates the CCS cost in Japan, which can be considered as a case study for specific countries where offshore sites are more suitable for CO₂ storage than onshore sites regarding geological reasons and barrier reduction of public/political acceptance. With the phasedown of unabated coal power, retrofitting amine-based post-combustion CO₂ capture system is a realistic way for pulverized coal-fired power plants. Capture cost was determined by the process simulation of coal-fired power plant retrofits. Current political realities in Japan suggest that CO₂ transport will be done by ship. Transport cost was estimated via a bottom-up analysis of each sub-process. Injection and monitoring cost was based on the values reported by the Tomakomai demonstration project, which are applicable to onshore injection into an offshore storage site. We find the full chain CCS cost to be 99–111 USD/t-CO₂. Though changing the solution in the CO₂ capture process from monoethanolamine to the blend of 2-amino-2-methyl-1-propanol and piperazine reduces the regeneration energy by 0.85 GJ/t-CO₂, the CCS cost was only reduced by ~9 USD/t-CO₂. Likewise, even when the regeneration energy was reduced to 2.0 GJ/t-CO₂ using a hypothetical amine solution embedded in a highly optimized PCC system, the CCS cost was still ~93 USD/t-CO₂. Considering that capital expenditure accounts for ~65% of capture cost, downsizing capture facilities may provide further cost reduction. Since transport and storage costs were roughly equivalent to capture costs, full chain CCS implementation is likely necessary to reduce costs through learning-by-doing, scale-out, and market effects.

Keywords : Economic analysis, Chemical absorption, Carbon neutral, Rate-based simulation, CO₂ avoided cost

1. Introduction

In 2020, the Japanese government declared a target of net zero emission of greenhouse gases by 2050 (Prime Minister of Japan and His Cabinet, 2021), with carbon capture and storage (CCS) as an essential technology to realize the target (METI, 2021a). The CCS process consists of three subprocesses: capture of CO₂ ('capture'), transport of captured CO₂ to a storage site ('transport'), and injection and monitoring of CO₂ ('storage'). The linkage of these technologies (termed: 'full chain') is necessary to realize CO₂ emissions reductions. Notably, there are multiple technological options to realize each sub-process, with the 'optimal' option being case-dependent. For example, in North America, onshore storage sites are abundant, and an existing CO₂ pipeline network provides relatively low-cost transport (GCCSI, 2021). On the other hand, in Europe and Japan, the potential storage sites are primarily offshore, making shipping of CO₂ more feasible than pipelines (Baroudi et al., 2021).

Despite the abundance of technological solutions available, CCS has not been deployed at the rate expected by modelers (Peters et al., 2017) or required by pledges of CO₂ emissions reductions (Wang et al., 2021). It is often stated that the main barrier hindering the rapid implementation of CCS is its high cost. Naturally, if the price of polluting (e.g.,

carbon price) is less than the cost of implementing CCS, then no company can be expected to choose the later. While carbon prices have climbed recently (Intercontinental Exchange, 2021), increasing the cost of polluting relative to the cost of CCS through research and development will only help to expedite CO₂ emissions reductions. The cost structure of CCS contains capital costs (CAPEX) and operating costs (OPEX) which are determined by the mix of technologies used to create the CCS chain, case-specific engineering decisions (e.g., CO₂ capture rate, CO₂ transport mass flow rate), and factors outside of the control of engineers (e.g., fuel price). As such, the full chain CCS cost should be evaluated at a national to regional-level, accounting for engineering, geographical, and political realities at a minimum.

Despite the inherent requirement of transport and storage to realize CO₂ emissions reductions, many cost analyses of CCS seem to focus only on the CO₂ capture process (Abu-Zahra et al., 2007; Feron et al., 2020) or assume simplified transport and storage costs without analysis of the interdependence between the subprocesses (Zoelle et al., 2015; GCCSI, 2017). Such analyses often assume particularly cheap transport and storage costs (e.g., 7–11 USD/t-CO₂); this reduces the full chain CCS cost and makes the capture cost appear relatively important. Recently, this discrepancy in the quality and depth of cost analysis has become apparent with more detailed, bottom-up analyses such as Psarras et al. (2020) finding that CCS cost is highly-dependent on the transportation mode, transportation distance, and storage methodology. Even with these promising improvements in full chain CCS analysis, there remains a dearth of case-specific cost analyses for CCS with offshore transport and storage.

This study estimates the cost of full chain CCS in Japan as a model case of countries without geologically or politically viable onshore CO₂ transport or storage sites. In the capture process, CO₂ removal from supercritical coal-fired pulverized power plant (PCPP) via chemical absorption using aqueous amine solutions is considered. In Japan, PCPP are the largest CO₂ emission source in power sector and represent a large risk of stranded assets in the face of Japan's net zero emissions pledge. Given the write-down of nuclear power assets following the Fukushima Daiichi nuclear accident, power companies will have difficulty in absorbing a complete shuttering of PCPP units. Being the most mature post-combustion CO₂ capture (PCC) technology, amine-based chemical absorption is chosen for evaluation. In the research field of amine-based PCC, much effort has been put into developing new amine and its blends to reduce the regeneration energy in the PCC process (Feron et al., 2020). We take this bottom-up analysis as an opportunity to assess the influence of the regeneration energy on the cost of full chain CCS. We evaluate a PCC system using the old-school gold standard amine solution (i.e., 30wt% monoethanolamine: MEA) and the new-school gold-standard (i.e., 27wt% 2-amino-2-methyl-1-propanol and 13wt% piperazine: AMP-PZ) (Feron et al., 2020). We further include evaluation of a hypothetical PCC system which can almost achieve the thermodynamically minimum regeneration energy.

2. Methods

2.1 Assumed CCS chain

Figure 1a), b), and c) provides a map of thermal power plants and potential storage area in Japan (Ministry of the Environment, 2021a). Though this analysis focuses on PCPP, CO₂ storage sites are likely to be shared between emitters; therefore, proximity to the aggregate of major point source emitters is likely to influence where CO₂ storage occurs. As shown in Fig. 1a), most of thermal power plants are located near coastlines but remote from potential subseafloor storage sites. Japanese law requires approval from each prefecture for the construction and operation of a pipeline (METI, 2021b). The seismically active nature of Japan suppresses positive pipeline construction in comparison with the central US, Canada, and Australia (Baroudi et al., 2021). The relative lack of pipelines in Japan may to some degree be explained by these political and geological realities. Taking these into account, we have selected shipping as a practical option to transport CO₂ in Japan. Note that the coastlines are highly complicated and that many gulfs or islands are scattered as shown in Fig. 1b) and c), making the ships meander.

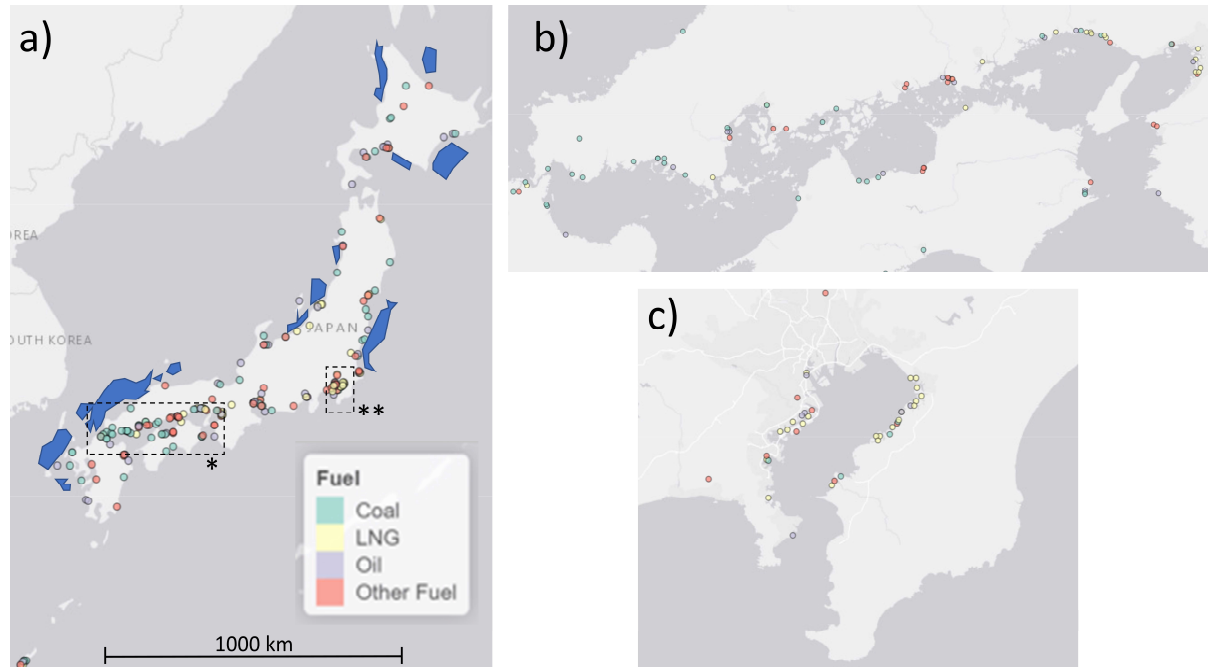


Fig. 1a) Map of thermal power plants in Japan (dots) and potential storage areas (blue regions), b) the enlarged view of the northern Kyushu, Setouchi, and western Kansai area represented as '*' in Fig. 1a), and c) the enlarged view of southern Kanto area represented as '***' in Fig. 1a).

Figure 2 shows the technologies chosen to create the CCS chain in this study. The logic supporting PCPP as the emission source was provided in section 1. Given the recent trends of project cancellation for new build coal-based power and the need to firm the grid against a growing share of renewable energy sources (METI, 2021a), we have selected PCPP retrofitted with PCC as a potential CCS pathway in Japan. It was assumed that the captured CO₂ from the PCC facility is non-pressureized and is sent to the onshore ‘export terminal’ of captured CO₂ via a short-distance onshore pipeline. The export terminal consists of a liquefaction plant, an intermediate storage tank, and facilities for loading CO₂ onto ships, and its capacity is 5.67 million tonnes per year in accordance with the PCPP capacity. As a baseline scenario, transport distance between the export terminal and the onshore ‘import terminal’ of transported CO₂ was set to be 1,000 km. The import terminal consists of equipment to unload CO₂ from ships, an intermediate storage tank, a CO₂ conditioning facility, and a CO₂ injection facility with multiple injection wells, and its capacity is the same as the export terminal. The CO₂ injection was assumed to be operated onshore into a subseafloor geological formation as demonstrated in the JCCS Tomakomai project (METI, 2020). In the following sections, cost estimation methodology for CO₂ capture, transport, and storage are explained in detail.

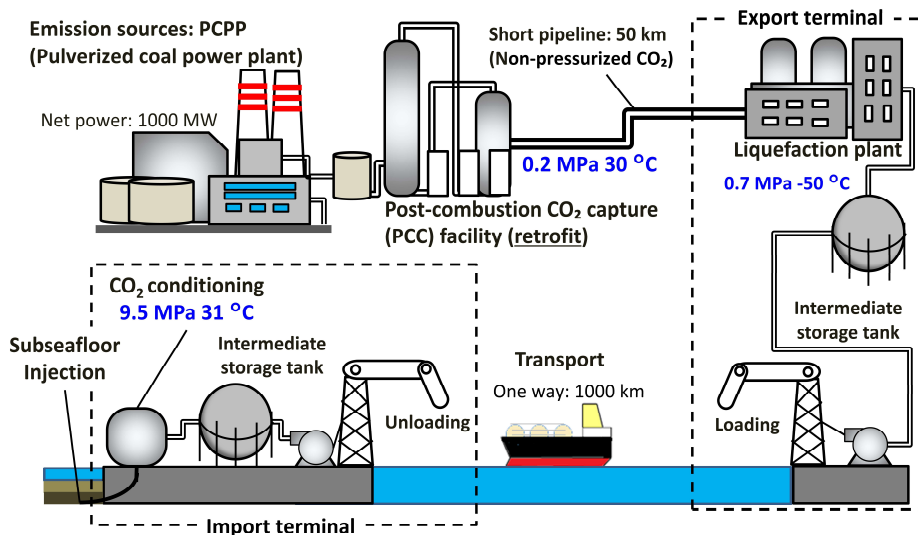


Fig. 2 CCS chain used in this study.

2.2 CO₂ capture method and cost

The CO₂ capture cost was calculated from the cost of electricity (COE) with and without retrofit PCC. To estimate the COE and CO₂ capture cost, process performance indices (e.g., fuel consumption rate, gross power output, and auxiliary load) were needed. These results were obtained using the commercial process simulator Aspen Plus® along with several auxiliary power estimation referencing Zoelle et al. (2015).

2.2.1 PCPP configuration and modelling

Using the commercial process simulator Aspen Plus®, a model of a 1,000 MW net power output PCPP without PCC was developed based on the report of the US DOE National Energy Technology Laboratory (NETL) (Zoelle et al., 2015). The PCPP model consists of several sub-processes: boiler, steam turbines, condenser, feedwater system, selective catalytic reduction (SCR), baghouse, flue gas desulfurization (FGD), and boiler feed pump turbine drives (BFPTD). Figure 3a) shows the process flow diagram (PFD) of the PCPP system; examples of the boiler and steam turbine subprocesses are provided in Fig. 3b) and Fig. 3c), respectively. As shown in Table 1, the configuration and operating conditions of the PCPP are based on current generation PCPP designs used in Japan; the main steam condition was set to 25.4 MPa and 607 °C while the reheated steam condition was set to 4.87 MPa and 605 °C. Other configuration and operating conditions (e.g., split fraction of steam extracted for feedwater heating, low pressure turbine inlet pressure) were basically set to the same value as the NETL report with a few minor modifications. The fuel used in this study was ‘Bituminous Illinois No.6’; its higher heating value (HHV) is 27,113 kJ/kg (Zoelle et al., 2015). Gross electrical power output was calculated from the irreversible adiabatic heat drop in the turbines. Auxiliary electric power consumption computable in Aspen Plus® (e.g., induced fan, primary fan, feedwater pump) was calculated within the simulation. Auxiliary power that cannot be computed in Aspen Plus® (e.g., pulverizer, FGD) was calculated using the estimation values of the NETL report. In the report, the mass flow rate of the main material streams was reported, and auxiliary power required for the main facilities were estimated. Using these values and the mass flow rate of the main material streams in this study, we estimated the auxiliary power; we approximated that the required electric power relevant to the feedwater system (e.g., cooling tower) are proportional to the main steam flow rate and that electric power relevant to fuel use and treatment (e.g., pulverizer, FGD) are proportional to the fuel consumption rate. The main steam flow rate, and necessary adjustment of fuel consumption rate, were set to achieve a net electrical power output of 1,000 MW. At the rated condition, the main steam flow rate was 2,840 tonne/hour and the fuel consumption rate was 91.22 kg/s.

Table 1 Configurations for the PCPP system.

	Units	
Gross power output	MW	1,049
Net power output	MW	1,000
Auxiliary power	MW	49
Fuel type		Bituminous Illinois No.6
Fuel higher heating value (HHV)	kJ/kg	27,113
Fuel consumption rate	kg/s	91.22
Net power efficiency	%	40.4
Steam temperature (main, reheated)	°C	607, 605
Steam pressure (main, reheated)	MPa	25.4, 4.87
Main steam flow rate	Tonne/hour	2,840

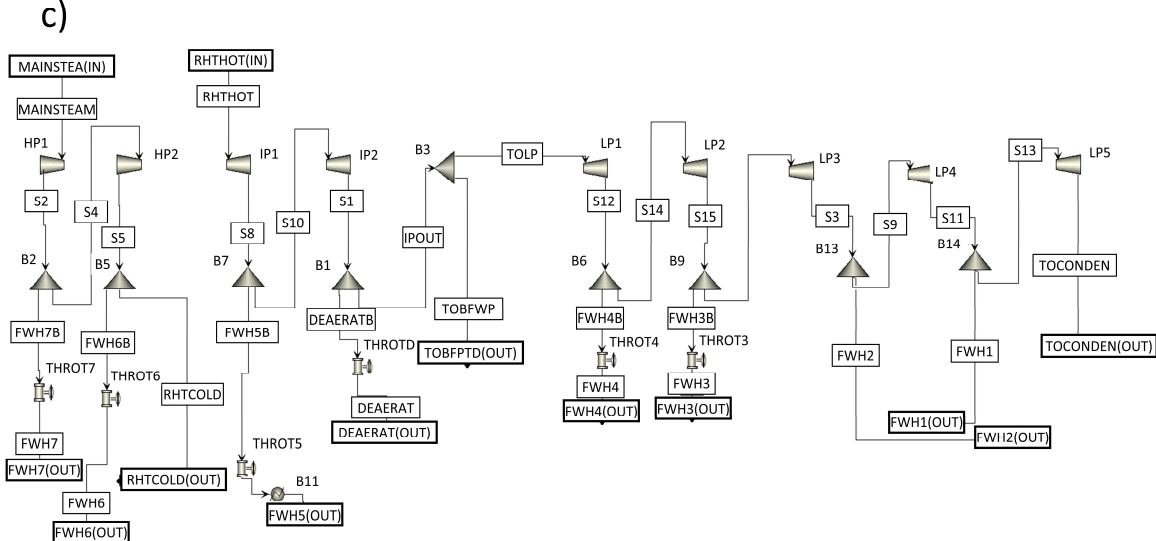
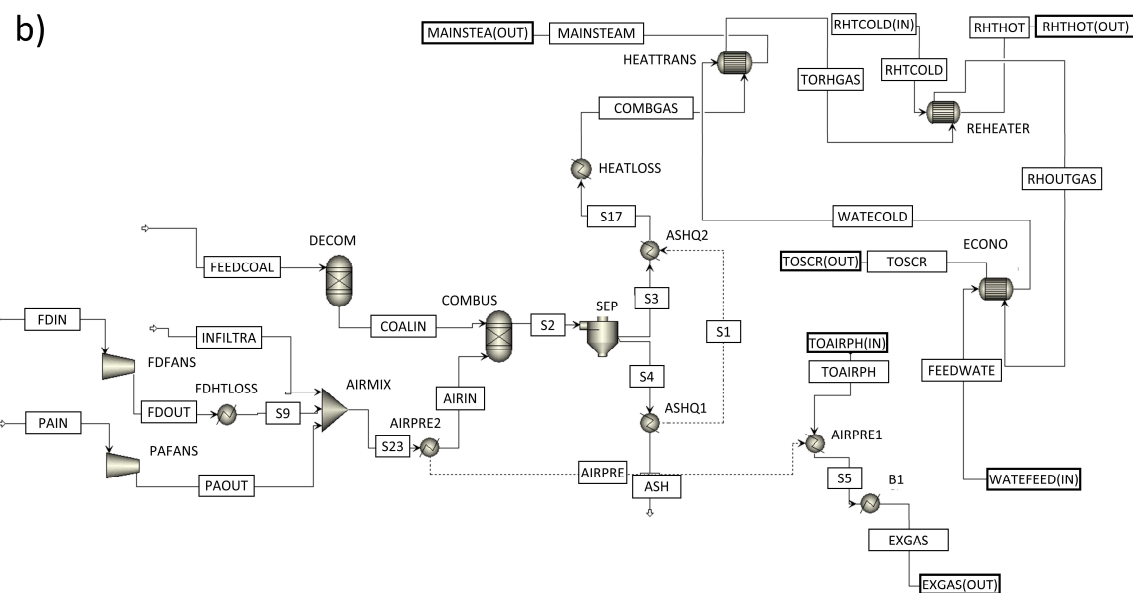
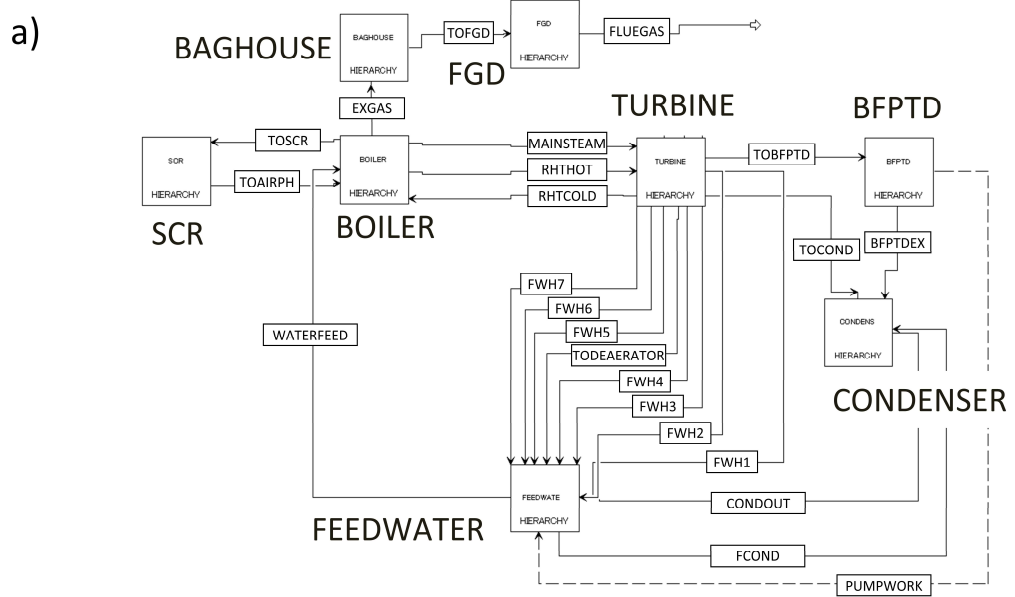


Fig. 3 Process flow diagram of a) the overall PCPP system, b) the boiler sub-process, and c) the steam turbines.

2.2.2 Modelling of aqueous amine solution in PCC

Prior to modelling amine-based PCC, solution property models of MEA and AMP-PZ were established based on the “ENRTL-RK_Rate_Based_MEA_model” and “ENRTL-RK_Rate_Based_PZ/MDEA_model” provided within Aspen Plus®, respectively (Aspen Technology, 2008a; Aspen Technology, 2008b). These built-in models apply the pure component database ‘PURE36’. For the AMP-PZ model, N-Methyldiethanolamine (MDEA) and its ion species were removed, and AMP and its ion species were added. The parameters related to following physical properties of AMP were obtained from Aspen Technology (2008c): viscosity, density, surface tension, heat of vaporization, specific heat capacity, dielectric constant, vapor pressure, and Henry’s constant for CO₂ in AMP. Table 2 provides chemical reactions in each model.

The chemical equilibrium constant (K_j) for reaction j in Eqs. (1)–(12) in Table 2 was calculated from the change of Gibbs free energy (ΔG_j°), ideal gas constant (R), and temperature (T) as written in Eq. (15). Calculation of ΔG_j° was done using the thermodynamic properties (i.e., standard enthalpy of formation, standard Gibbs free energy of formation, specific heat capacity) in Aspen Plus® (Aspen Technology, 2008a; Aspen Technology, 2008b). For the chemical reactions of Eqs. (13) and (14), the K_j was calculated using the correlation of Eq. (16) due to the poor accuracy of the vapor liquid equilibrium prediction of the AMP aqueous solution provided by Aspen Plus® (Aspen Technology, 2008c). The constants A – D in Eq. (16) are provided in Table 3. The chemical equilibrium constant given by Tong et al. (2012) was converted from molality to a mole fraction basis. Interaction parameters used in the electrolyte non-random two-liquid (eNRTL) model, which calculates the activity coefficient of each chemical species in the system, were given as follows: the values in the PZ/MDEA example file were used for molecule-molecule and molecule-ion pair parameters which include only species present in Eqs. (6)–(12), the values reported by Hartono et al. (2020) were used for molecule-molecule and molecule-ion pair parameters which include only species present in Eqs. (6)–(8) or (13)–(14). In addition to the above alterations, some parameters were determined by fitting to more accurately predict published data of the solution properties. The list of modified parameters was shown in Isogai and Nakagaki (2022) along with model validation via experimental data for AMP-PZ aqueous solutions. For the MEA model, the parameters given by Aspen Plus® (Aspen Technology, 2008a) were used without modification.

Table 2 Chemical reactions in the simulation model.

Model	Reaction	Eq. Number
MEA	2 H ₂ O <--> H ₃ O ⁺ + OH ⁻	(1)
	CO ₂ + OH ⁻ <--> HCO ₃ ⁻	(2)
	HCO ₃ ⁻ + H ₂ O <--> CO ₃ ⁻² + H ₃ O ⁺	(3)
	MEAH ⁺ + H ₂ O <--> MEA + H ₃ O ⁺	(4)
	MEA + CO ₂ + H ₂ O <--> MEACOO ⁻ + H ₃ O ⁺	(5)
AMP-PZ	2 H ₂ O <--> H ₃ O ⁺ + OH ⁻	(6)
	CO ₂ + OH ⁻ <--> HCO ₃ ⁻	(7)
	HCO ₃ ⁻ + H ₂ O <--> CO ₃ ⁻² + H ₃ O ⁺	(8)
	PZH ⁺ + H ₂ O <--> PZ + H ₃ O ⁺	(9)
	PZ + CO ₂ + H ₂ O <--> PZCOO ⁻ + H ₃ O ⁺	(10)
	PZCOO ⁻ + HCO ₃ ⁻ <--> PZ(COO ⁻) ₂ + H ₂ O	(11)
	H ⁺ PZCOO ⁻ + H ₂ O <--> PZCOO ⁻ + H ₃ O ⁺	(12)
	AMPH ⁺ + H ₂ O <--> AMP + H ₃ O ⁺	(13)
	AMP + CO ₂ + H ₂ O <--> AMPCOO ⁻ + H ₃ O ⁺	(14)

Table 3 Chemical equilibrium constant on mole fraction basis used in this model.

Eq. Number	A	B	C	D	Source
(13)	300.46	-7625.01	-43.6376	0	(Tong et al., 2012)
(14)	-14.0057	2623.74	-1.8581	0	(Hartono et al., 2020)

$$\ln K_j = -\frac{\Delta G_j^\circ}{RT} \quad (15)$$

$$\ln K_j = A + \frac{B}{T} + C \cdot \ln T + D \cdot T \quad (16)$$

2.2.3 PCC configuration and modelling

Figure 4 shows the PFD of the amine-based PCC system modelled using Aspen Plus®. The CO₂ absorption in the absorber and the desorption in the stripper were calculated by the Aspen Ratesep™ rate-based model. Table 4 provides the configurations for the absorber and the stripper, along with the operating conditions in the PCC process simulation. The column diameter was determined to keep the flooding factor below 80%. The structured packing ‘Mellapak 250Y’ was used for both columns in accordance with recommendations in IEAGHG (2012). The temperature difference at the cold side of the heat exchanger was assumed to be 5 K. The liquid to gas ratio (L/G) was varied as an operating parameter, and the liquid flow rate was varied corresponding to L/G in Table 4. By adjusting the pressure of the stripper according to the change in the liquid flow rate, the temperature at the bottom of the stripper was fixed to 122 °C to mitigate thermal degradation of the amine solution. The CO₂ capture rate was held constant at 90% by adjusting the reboiler duty. Regarding chemical reactions, while reactions in the stripper can be regarded as instantaneous and reach equilibrium due to high temperature (Van Wagener, 2011), some reactions in the absorber must be regarded as a kinetically controlled. For the MEA model, the kinetically controlled reactions and parameters given in Aspen Plus® (Aspen Technology, 2008a) were used without any alteration in the absorber calculation. For AMP-PZ model, the kinetically controlled reactions and parameters in Table 5 were included and used in the absorber calculation. The reactions listed in Table 5 replace chemical reactions with the same reaction number in Table 2. The power law expression of Eq. (17) was used to calculate reaction rates when the reference temperature (T_0) is specified in Table 5. When T_0 is not specified, Eq. (18) was used instead. In Eqs. (17) and (18), r_j is the reaction rate for reaction j in kmol/(m³·s), k_j^0 is the pre-exponential factor in m³/(kmol·s) (molarity basis) or kmol/(m³·s) (mole gamma basis), E_j is the activation energy for reaction j in kJ/kmol, R is the ideal gas constant in kJ/(kmol·K), T is the system temperature in K, T_0 is in K, C_i is the molarity of species i in kmol/m³ (molarity basis) or the activity of species i (mole gamma basis), and a_{ij} is the reaction order of species i for reaction j .

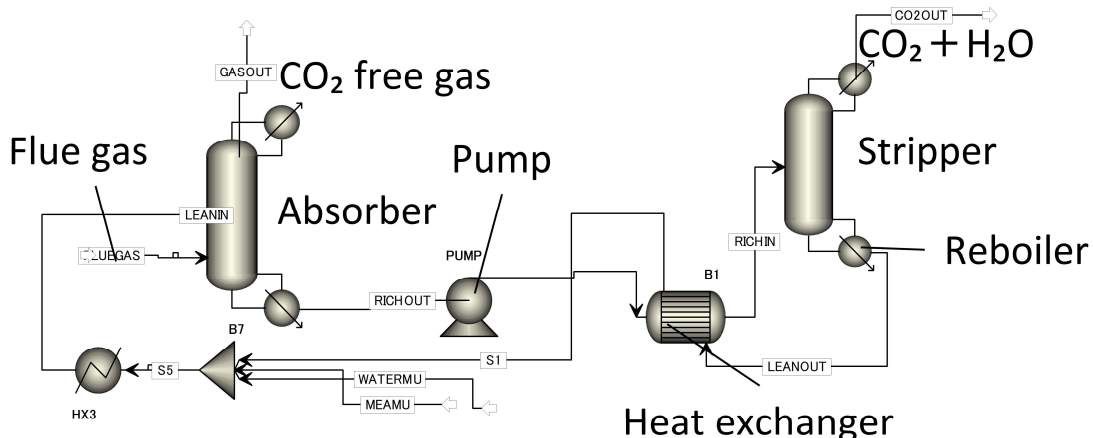


Fig. 4 Process flow diagram of the amine-based PCC simulation model in Aspen Plus®.

Table 4 Configurations for the absorber and the stripper, and operational conditions in PCC process simulation.

	Units	
Packing height (absorber, stripper)	m	40, 30
Column inner diameter (absorber, stripper)	m	25, 17
Packing type (absorber, stripper)	-	Mellapak 250Y, Mellapak 250Y
Temperature at the absorber inlet (liquid, gas)	°C	40, 40
Liquid temperature at the stripper outlet	°C	122
Pressure in the column (absorber, stripper)	kPa	101.325, Adjusted
Liquid-to-gas ratio	MEA AMP-PZ	3.53, 3.98, 4.52 1.83, 2.01, 2.57

$$r_j = k_j^0 \exp \left\{ -\frac{E_j}{R} \left(\frac{1}{T} - \frac{1}{T_0} \right) \right\} \prod C_i^{a_{ij}} \quad (17)$$

$$r_j = k_j^0 \exp \left(-\frac{E_j}{RT} \right) \prod C_i^{a_{ij}} \quad (18)$$

Table 5 Kinetically controlled reactions in the absorber and kinetic parameters for AMP-PZ model.

	Eq.* ¹	k^0	E kJ/kmol	T_0 K	C_i basis	Source
$\text{CO}_2 + \text{OH}^- \rightarrow \text{HCO}_3^-$	(7f)	1.33×10^{17}	5.547×10^4	-	Mole gamma	*2
$\text{HCO}_3^- \rightarrow \text{CO}_2 + \text{OH}^-$	(7b)	6.63×10^{16}	1.074×10^5	-	Mole gamma	*2
$\text{PZ} + \text{CO}_2 + \text{H}_2\text{O} \rightarrow \text{PZCOO}^- + \text{H}_3\text{O}^+$	(10f)	5.37×10^4	3.36×10^4	298.15	Molarity	*3
$\text{PZCOO}^- + \text{H}_3\text{O}^+ \rightarrow \text{PZ} + \text{CO}_2 + \text{H}_2\text{O}$	(10b)	2.490×10^9	7.022×10^4	298.15	Molarity	*4
$\text{PZCOO}^- + \text{CO}_2 + \text{H}_2\text{O} \rightarrow \text{PZ}(\text{COO}^-)_2 + \text{H}_3\text{O}^+$	(11f)	4.7×10^4	3.36×10^4	298.15	Molarity	*5
$\text{PZ}(\text{COO}^-)_2 + \text{H}_3\text{O}^+ \rightarrow \text{PZCOO}^- + \text{CO}_2 + \text{H}_2\text{O}$	(11b)	3.289×10^{10}	5.115×10^4	298.15	Molarity	*6
$\text{AMP} + \text{CO}_2 + \text{H}_2\text{O} \rightarrow \text{AMPCOO}^- + \text{H}_3\text{O}^+$	(14f)	1.94×10^{10}	4.3×10^4	-	Molarity	*7
$\text{AMPCOO}^- + \text{H}_3\text{O}^+ \rightarrow \text{AMP} + \text{CO}_2 + \text{H}_2\text{O}$	(14b)	6.811×10^{22}	7.334×10^4	-	Molarity	*8

*1 ‘f’ and ‘b’ mean forward and backward, respectively. *2 Aspen Technology, 2008b. *3 Bishnoi and Rochelle, 2000.

*4 Parameters determined from the kinetics of (10f) and the equilibrium constant of this reaction. The equilibrium constant was obtained by the combination of equilibrium constants of following reactions: PZ carbamate formation (Ermatchkov et al., 2003), dissociation of water to proton and hydroxide ion (Edwards et al., 1978), dissociation of CO_2 to bicarbonate ion (Edwards et al., 1978), and dissociation of water to oxonium ion and hydroxide ion (Posey and Rochelle, 1997). *5 Bishnoi and Rochelle, 2002. *6 Parameters determined from the kinetics of (11f) and the equilibrium constant of this reaction. As with *4, the equilibrium constant was obtained using the reaction equilibrium constant of PZ dicarbamate formation (Ermatchkov et al., 2003) instead of PZ carbamate formation. *7 Saha et al., 1995. *8 Parameters determined from the kinetics of (14f) and the equilibrium constant of this reaction. As with *4, the equilibrium constant was obtained using the reaction equilibrium constant of AMP carbamate formation (Silkenbäumer et al., 1998) instead of PZ carbamate formation.

2.2.4 PCC integration and whole system operating condition

The PCC facility was installed downstream of the FGD system. The PCC reboiler heat duty to recover CO_2 from rich amine solution was provided by the steam extracted from the crossover pipe between the intermediate pressure (IP) and the low pressure (LP) turbines. Since the steam extraction decreases the power output of PCPP retrofitted with PCC, this study assumed that up to 110% of the main steam flow rate at the original rated condition was admissible to recompense power output deficiency. The corresponding increase in the fuel mass flow rate and other associated operational changes were accounted for in the model. To prevent providing excessively high temperature steam to the reboiler, the steam extracted from the IP/LP crossover (270°C , 510 kPa) was expanded in an auxiliary turbine for power recovery and de-superheated via an attemperator to 134°C and 295 kPa prior to introduction to the reboiler. The steam extraction reduces the pressure at the IP/LP crossover, leading to an increased loading of the exhaust stage of the IP turbine. To mitigate this effect, a pressure maintaining valve was installed upstream of the LP turbine inlet. The pressure drop at this valve was calculated by the Ellipse law (Lucquiaud, 2010).

While PCPP-PCC system performance using existing amine solutions (i.e., MEA and AMP-PZ) was evaluated by combining the PCPP model in section 2.2.1 and PCC model in section 2.2.3, the performance of hypothetical PCPP-PCC (‘hypothetical PCC’) system which can achieve the regeneration energy of 2.0 GJ/t- CO_2 with a hypothetical solution was evaluated without using the detailed calculations of the PCC model. The regeneration energy in the PCC consists of heat of CO_2 desorption, heat of water vaporization, and the sensible heat of the solution. While the heat of water vaporization and the sensible heat can be reduced by the amine solution with high-performance or heat recovery management, the heat of CO_2 desorption cannot be dispensed in any case. Ultimately, the regeneration energy can be approximated by only the heat of CO_2 desorption of the amine solution excluding sensible heat and heat of water vaporization. According to this approximation, the regeneration energy of 2.0 GJ/t- CO_2 corresponds to the heat of CO_2 desorption of 90 kJ/mol- CO_2 . This value can be regarded as relatively low and feasible by reviewing the heat of CO_2 desorption of various amine solutions; the heat of CO_2 absorption at 120°C (\approx heat of CO_2 desorption) for most of the amine solutions is more than 90 kJ/mol- CO_2 (Kim and Svendsen, 2011). Though some amine solutions such as the blend of potassium carbonate and piperazine have the lower heat of CO_2 desorption and seems to be favorable, such solutions have relatively lower CO_2 partial pressure at the stripper temperature, leading to the increase in the heat of water vaporization (Oexmann and Kather,

2010). It has been a common understanding that lower heat of CO₂ desorption does not necessarily reduce the overall regeneration energy (Oexmann and Kather, 2010; Rochelle et al., 2011). As such, the regeneration energy of 2.0 GJ/t-CO₂ defined in this study seems to be appropriate as a target for the next-generation PCC system. Then, the required steam extraction to the reboiler was determined from the defined regeneration energy and the same CO₂ mass flow rate captured as the MEA and AMP-PZ cases. The auxiliary power consumption in the ‘hypothetical PCC’ (e.g., amine solution feed pump, flue gas blower) was assumed to be the same as that in the AMP-PZ case. The other calculations were performed in the same manner as the cases employing MEA and AMP-PZ.

2.2.5 Cost of electricity, capture cost, and CO₂ avoided cost

The cost of electricity (COE) with and without PCC was calculated following the method by US DOE (Theis, 2019). The COE was estimated as a function of the annual CAPEX, fixed OPEX (OC_{FIX}), variable OPEX (OC_{VAR}), capacity factor (CF), and net electrical power output (MW) as written in Eq. (19). For CAPEX, the Bare Erected Cost (BEC) was calculated based on the following three facilities: a 580 MW gross output PCPP without PCC (reported as “B12A” in Zoelle et al., 2015), a PCC system retrofitted to a 580 MW gross output PCPP (reported as “Case 0” in Chou et al., 2016), and auxiliary equipment for PCC retrofit to a 580 MW gross output PCPP (same as the above). Location factors relevant to Japan were applied to modify the BEC estimation (Japan Machinery Center for Trade and Investment, 2012). Next, the modified BEC were converted to a 2020 basis by applying relevant plant cost indices (Japan Machinery Center for Trade and Investment, 2012; Japan Machinery Center for Trade and Investment, 2020). The BEC were further converted to the Total Plant Cost (TPC), with the “0.6 rule” (Tribe and Alpine, 1986) applied to scale-up of the three reference facilities to the 1,000 MW plant modelled in this study. The TPC was then converted to the Total Overnight Cost (TOC) in Eq. (19) by adding the inventory cost, owner’s cost, and similar ancillary costs to the TPC. The TOC depends on whether the thermal power plant’s CAPEX depreciation period has ended or not. In this study, we report two costs: ‘during’ and ‘after’ the PCPP CAPEX depreciation period. The TOC ‘during’ PCPP CAPEX depreciation was determined by including the TPC of all three facilities above mentioned. The TOC ‘after’ PCPP CAPEX depreciation was determined by excluding the TPC of the PCPP. A weight average retrofit factor was applied to the TOC to account for the retrofit cost premium (Chou et al., 2016). The TOC was converted to Total As-Spent Capital (TASC) via the conversion factor in Theis et al. (2019). The TASC represents the sum of all capital expenditures. The TASC was converted to the annual CAPEX by multiplying by the fixed charge rate (FCR) (Theis, 2019).

For fixed OPEX, the operating labor costs provided by the US DOE report were used and other relevant costs (e.g., maintenance labor, insurance) were calculated from TPC cost based on the method in Zoelle et al. (2015). The fuel coal and consumables for flue gas treatment are large portion of variable OPEX. The consumption rate of consumables for flue gas treatment is proportional to the flue gas flow rate and the flue gas flow rate is proportional to fuel consumption rate. Therefore, the consumption rate of consumables for flue gas treatment can be assumed to be proportional to the fuel consumption rate. In the US DOE report (Zoelle et al., 2015), the fuel consumption rate was reported, and the cost of consumables for flue gas treatment was estimated. Using these values and the fuel consumption rate calculated by Aspen Plus® simulation in this study, we estimated the cost of consumables for flue gas treatment; we approximated that the cost of consumables is proportional to the fuel consumption rate. For fixed OPEX, the wage index for all industries was used. For variable OPEX, the Producer Price Index for ‘chemicals & related products’ was applied (Japan Machinery Center for Trade and Investment, 2020). For fuel cost, the average price of coal imported to Japan in 2020 was used (Trade Statics of Japan, 2021). Net electrical power output was calculated based on the Aspen Plus® process simulation results.

The CO₂ capture cost and CO₂ avoided cost were calculated using Eqs. (20) and (21), respectively. Table 6 summarises key parameters for COE calculation used in this study. Note that the CO₂ emissions_{w/CCS} in Eq. (21) does not include the CO₂ emission from transport and storage in accordance with the US DOE report (Zoelle et al., 2015). The cost in this study was calculated as 2020 Japanese yen basis and converted to 2020 US dollar basis by the exchange rate (Japan Machinery Center for Trade and Investment, 2020).

$$\text{COE [USD/kWh]} = \frac{\text{FCR} \cdot (\text{TASC}/\text{TOC}) \cdot \text{TOC} + \text{OC}_{\text{FIX}} + \text{CF} \cdot \text{OC}_{\text{VAR}}}{\text{CF} \cdot 8760 \cdot \text{MW}} \quad (19)$$

$$\text{CO}_2 \text{ capture cost [USD/t-CO}_2\text{]} = \frac{(\text{COE}_{w/\text{PCC}} - \text{COE}_{w/o\text{ PCC}}) [\text{USD/kWh}]}{\text{CO}_2 \text{ captured [t-CO}_2/\text{kWh}]} \quad (20)$$

$$\text{CO}_2 \text{ avoided cost [USD/t-CO}_2\text{]} = \frac{(\text{COE}_{w/\text{CCS}} - \text{COE}_{w/o\text{ CCS}}) [\text{USD/kWh}]}{(\text{CO}_2 \text{ emissions}_{w/o\text{ CCS}} - \text{CO}_2 \text{ emissions}_{w/\text{CCS}}) [\text{t-CO}_2/\text{kWh}]} \quad (21)$$

Table 6 Key parameters for COE calculation.

		Value
Capacity factor		0.85
TASC/TOC nominal		1.289
Nominal fixed charge rate		0.0886
Location factor in 2011 (Japan/USA)	Material, Equipment Construction Indirect	1.224 (= 58.4/47.7) 1.373 (= 22.8/16.6) 1.324 (= 9.8/7.4)
Weighted average retrofit factor		1.1
Exchange rate JPY/USD (2011, 2020)		79.8, 107.3
Coal price (2020) JPY/MT		8,724
Plant cost index ratio (2020/2011)	Equipment Construction Indirect	1.049 (= 160.2/152.7) 1.281 (= 168.8/131.8) 1.087 (= 127.1/116.9)
Fixed OPEX cost index ratio (2020/2011)		1.018 (= 101.7/99.9)
Variable OPEX cost index ratio (2020/2011)		0.863 (= 88.9/103.0)

2.3 Transport method and cost

2.3.1 Transport process

As mentioned in section 2.1, this study assumed CO₂ transport via ship. Round-trip transport with a 1,000 km distance between the export terminal and the import terminal was set as the baseline scenario. Average shipping distance for CO₂ emissions from the thermal power plants in Japan is ~1,000 km when either of two promising storage sites (i.e., southern Hokkaido or northern Kyushu) are opened (see Fig. A1 in Appendix A). It was assumed that the CO₂ from the PCC facility is non-pressurized and is sent to the onshore export terminal via a short-distance (50 km) onshore pipeline. The export terminal consists of a liquefaction plant, an intermediate storage tank, and equipment for loading CO₂ onto ships. With regard to the size of the terminal, economies of scale to some degree (<5 Mtpa) leads to the cost reduction (Element energy, 2018), and ‘hub and cluster’ concept, which connects multiple emitters to a single export terminal, is attractive. However, its scale effect become limited beyond a certain point (e.g., 5 Mtpa) (IEAGHG, 2020). Since the CO₂ mass flow rate from a single PCPP in this study is large enough (=5.67 Mtpa), it was assumed that the export and import terminal is sized to fit this single PCPP. Since high density is preferable as a shipping condition, 0.7 MPa and -50 °C was selected which is near the triple point. To achieve this condition before loading to a ship, liquefaction is required. A combined internal and external cooling loop using NH₃ was assumed, with an electricity consumption of 134 kWh/t-CO₂ (IEAGHG, 2020). Before and after shipping transport, CO₂ intermediate storage and loading/unloading were assumed. From the operating parameters in Table 7, the cycle time of one round-trip was calculated. The number of ships required was calculated considering the cycle time, CO₂ mass flow rate, and safety margins in Table 7. The CO₂ mass flow rate was based on the PCC system. The import terminal consists of equipment to unload CO₂ from a ship, an intermediate storage tank, a CO₂ conditioning facility, and a CO₂ injection facility with multiple injection wells. For both the export terminal and the import terminal, the size of required intermediate storage tank was assumed to be the same as the cargo ship (50 kt-CO₂) following the method by IEAGHG (2020). After unloading and intermediate storage, the CO₂ conditioning (i.e., heating and pressurizing to 9.5 MPa and 31 °C) were performed. The required electricity power was calculated to be 2.71 kWh/t-CO₂ from process simulation using Aspen Plus®.

Table 7 Operating parameters relevant to logistics (IEAGHG, 2020).

	Units	
Transport distance (one-way)	km	1,000
Ship speed	knots	15
Loading rate (intermediate storage tank↔ship)	t-CO ₂ /h	3,000
Time to connect/disconnect ship	h	2
Weather margin		0.95
Operational margin		0.98

2.3.2 Transport cost

Cost of CO₂ transport was calculated by bottom-up analysis of each sub-process *i* as written in Eq. (22). In Eq. (22), net CO₂ transported was calculated by subtracting 2% of CO₂ for boil-off (IEAGHG, 2020) and CO₂ generated in several sub-processes (i.e., electric power for liquefaction and conditioning, ship fuel use) from captured CO₂. The CAPEX and OPEX of each sub-process was calculated considering CO₂ mass flow rate or facility capacity using parameters in Table 8. Annual CAPEX was calculated assuming a 20 years lifetime (IEAGHG, 2020). In Table 8, the values are 2018 € basis. Therefore, these values were converted to 2018 JPY, and then to 2020 JPY by applying the Producer Prices Index for all commodities (Japan Machinery Center for Trade and Investment, 2020). Finally, the costs were converted to 2020 USD. Variable OPEX, electricity power consumption for CO₂ liquefaction and conditioning, cooling water for CO₂ liquefaction, and fuel consumption for shipping were calculated using the assumptions in Table 9. For CO₂ liquefaction, the labour OPEX of 0.49 €/(t-CO₂/y) was also included in accordance with IEAGHG (2020). The short-distance (50 km) pipeline transport cost (0.61 USD/t-CO₂) was added to the shipping transport cost, which was calculated by FE/NETL CO₂ Transport Cost Model (NETL, 2018).

Table 8 CAPEX and OPEX assumptions for CO₂ transport facilities (IEAGHG, 2020).

	CAPEX	Units	OPEX % of CAPEX
Liquefaction	38.9	€/(t-CO ₂ /y)	4 *1
Intermediate storage	1,300	€/t-CO ₂ stored in tanker	5
Loading/Unloading	600	€/(t-CO ₂ /h)	6
Ship	75.91 *2	Million €	5
CO ₂ conditioning	4.21	€/(t-CO ₂ /y)	11

*1 Only fixed OPEX. *2 Calculated from corresponding fitting curves of construction cost as a function of ship cargo capacity (IEAGEG, 2020).

Table 9 OPEX assumptions for CO₂ transport.

		Units	Reference
Electricity cost (Liquefaction)	13.96	JPY/kWh	TEPCO Energy Partner, Inc., 2022 *1
Electricity cost (Conditioning)	14.40	JPY/kWh	TEPCO Energy Partner, Inc., 2022 *1
Cooling water	7.44	m ³ /t-CO ₂	IEAGHG, 2020
Cooling water cost	0.02	€/m ³	IEAGHG, 2020
Emission intensity (Electricity)	0.496	kg-CO ₂ /kWh	Ministry of the Environment, 2021b
Emission intensity (Class C fuel oil)	3.00	t-CO ₂ /t-fuel	Japan LP Gas Association, 2022
Ship fuel cost (Class C fuel oil)	37,063	JPY/m ³	Energy Information Center, 2021 *2
Ship fuel consumption rate*3	38.02	Tonne/day	Mitsubishi Heavy Industry, 2004

*1 Contract demand <10,000 kW: 14.4 JPY/kWh ; 10,000-50,000 kW: 14.18 JPY/kWh ; >50,000 kW: 13.96 JPY/kWh.

*2 Raw data by Japan Federation of Coastal Shipping Associations. *3 Capacity: 50 kt, Speed: 15 knots.

$$\text{Shipping transport cost[USD/t-CO}_2\text{]} = \sum_i \frac{(\text{CAPEX} + \text{OPEX}) [\text{USD/year}]}{\text{Net CO}_2 \text{ transported [t - CO}_2/\text{year}]} \quad (22)$$

2.4 Storage method and cost

For CO₂ storage, the injection was assumed to be operated from an onshore site to a subseafloor geological formation consistent with the JCCS Tomakomai CCS demonstration project. The cost estimated from Tomakomai demonstration project was used to estimate injection cost in this analysis (METI, 2020). The cost includes the CAPEX of injection wells

and monitoring wells, marine environment survey, and 3D elastic wave probe system. The marine environment survey is performed 4 times per year and 3D elastic wave probe system are performed 10 times in a 25 year span.

3. Results and discussion

3.1 Process performance and cost of CO₂ capture

Table 10 shows the process simulation results for PCPP performance in each of the system integrations explored in this study. The PCC simulation, a L/G of 3.98 for MEA and 2.01 for AMP-PZ were applied; these correspond to a minimization of the regeneration energy. Switching the amine solution in the PCC system from MEA to AMP-PZ reduced the regeneration energy by ~0.85 GJ/t-CO₂ and improved the plant efficiency by ~1.66%. Switching the PCC system from the one using AMP-PZ solution to the ‘hypothetical PCC’ reduced the regeneration energy by ~0.59 GJ/t-CO₂ and improved the plant efficiency by ~1.17%. These results are consistent with the linear trend between the regeneration energy and thermal power plant efficiency found by others; a 2% improvement in plant efficiency can be expected if the regeneration energy is reduced by 1 GJ/t-CO₂. (Goto et al., 2013). Due to 10% increase in the main steam flow rate and corresponding fuel consumption rate, PCPP integrated with PCC using AMP-PZ and ‘hypothetical PCC’ could maintain 96% and 99% of net power output of the unabated PCPP, respectively. Figure 5 shows the breakdown of COE excluding the cost of CO₂ transport and storage. The CAPEX and fuel cost were found to dominate the COE. Figure 5 also shows that the COE decreases dramatically after the PCPP CAPEX depreciation period; this indicates that PCPP retrofit with PCC might be a financially attractive option in particular if the PCPP CAPEX depreciation period has ended. Figure 6 shows the CO₂ capture cost excluding the cost of CO₂ transport and storage. The CO₂ capture cost is capital intensive in all instances, accounting for ~65% of the cost. Although improved amine solutions reduce the regeneration energy as shown in Table 10, the relative impact on the CO₂ capture cost is limited. Historically, much effort has gone into reducing the regeneration energy of amine solutions. Figures 5 and 6 suggest that research and development targeting CAPEX reduction provide more potential for further cost reductions. Large reductions in the CAPEX in PCC systems can be achieved by downsizing of the absorber, stripper, and heat exchanger. In particular, the absorber accounts for near the half of the CAPEX (Feron, 2016), and use of amine solution with high CO₂ absorption rate or advanced packing material geometries can reduce the height of absorber column.

Table 10 Pulverized coal thermal power plant system performance.

		without PCC	with PCC		
			MEA	AMP-PZ	Hypothetical PCC
CO ₂ capture rate	%	-	90.0	90.0	90.1
Gross output	MW	1,049.3	988.9	1,033.1	1,065.1
Auxiliary power	MW	49.6	75.9	75.1	75.1
Net output	MW	999.7	913.0	958.0	990.0
Plant efficiency (HHV)	%	40.42	33.56	35.22	36.39
CO ₂ captured	t/MWh	-	0.834	0.794	0.769
CO ₂ emission	t/MWh	0.779	0.092	0.088	0.086
Regeneration energy	GJ/t-CO ₂	-	3.44	2.59	2.00

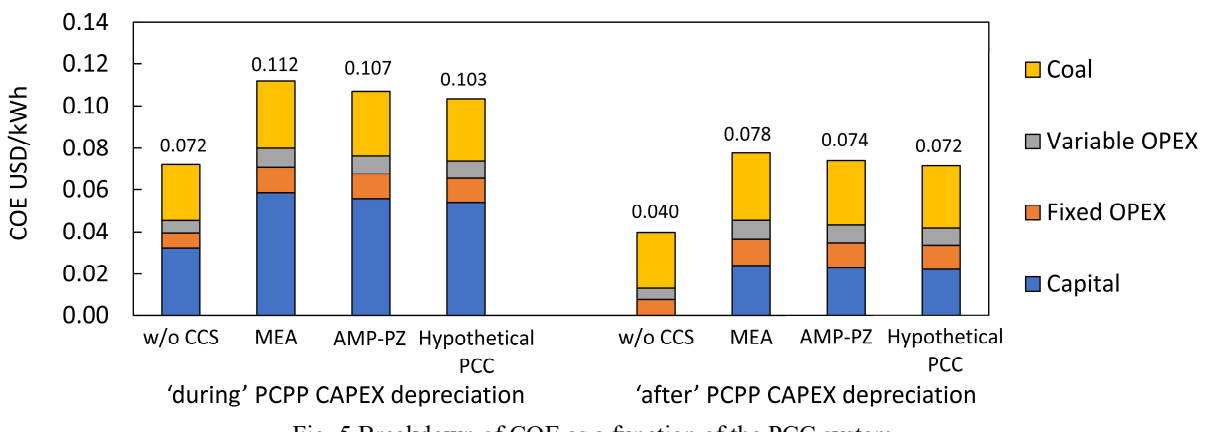


Fig. 5 Breakdown of COE as a function of the PCC system.

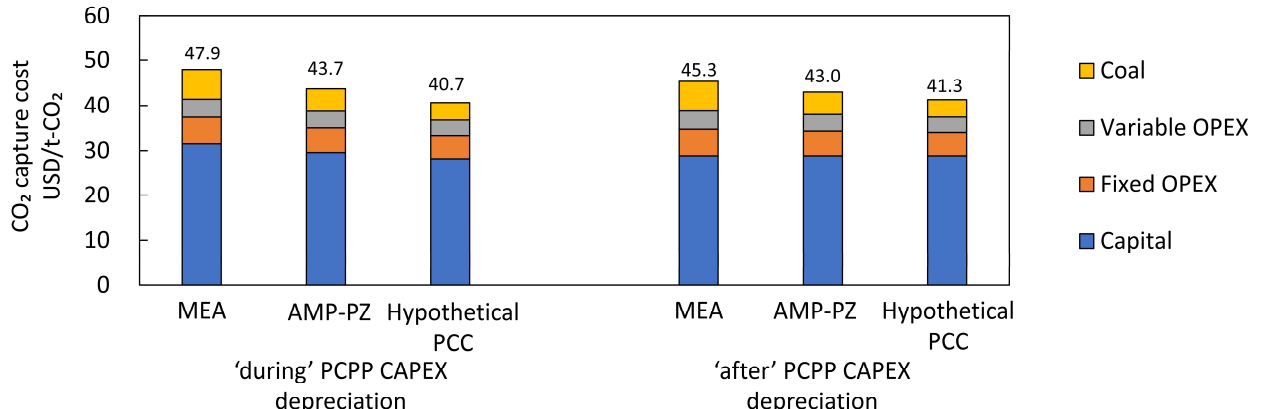


Fig. 6 Breakdown of CO₂ capture cost as a function of the PCC system.

3.2 Cost of CO₂ transport

Figure 7a) breaks down the activities comprising the 113-hour cycle time of a round-trip of the ship between the export terminal and the import terminal based on the conditions in Table 7. The CO₂ mass flow rate from the PCC facility was 5.67 Mt per year. In this study, two ships with the capacity of 50 kt-CO₂ were required. Figure 7b) breaks down the CO₂ transport cost into its specific activities and distinguishes between CAPEX and OPEX. The total cost of CO₂ transport was 33.43 USD/t-CO₂, with liquefaction and shipping being the key cost drivers. Since ~78% of liquefaction cost is due to the electricity for cooling and compressing CO₂, process modification to reduce the electricity power demand would provide substantial cost savings.

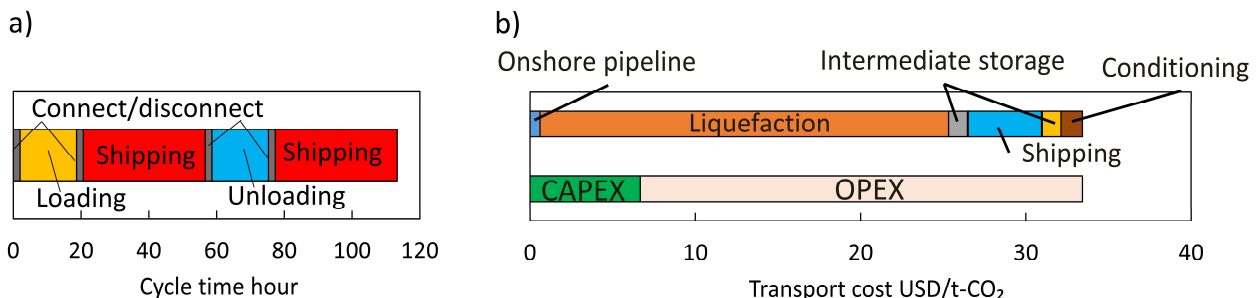


Fig. 7a) Cycle time of one round-trip of the ship and b) breakdown of CO₂ transport cost, divided into sub-processes (upper) and CAPEX and OPEX (lower). Note that the costs for loading and unloading are not labeled in Fig. 7b) due to the relatively small size of these sub-processes.

3.3 Cost of CO₂ storage

As mentioned in section 2.4, the cost estimated in the report of Tomakomai CCS demonstration project (METI, 2020) was used for the cost of storage and monitoring. The total cost of storage and monitoring was 14.1 USD/t-CO₂, and its allocation was the CAPEX of 3.4 USD/t-CO₂ and the OPEX of 10.7 USD/t-CO₂.

3.4 Full chain CCS cost

Figure 8 provides a breakdown of the full-chain CCS COE, which is a ~32% and ~46% increase over the capture-only COE in the case of 'during' and 'after' the PCPP CAPEX depreciation period, respectively. Figure 9 shows a breakdown of the full-chain CCS CO₂ avoided cost, which reaches 99–111 USD/t-CO₂ for PCC using existing amine solutions (i.e., MEA and AMP-PZ). From Fig. 9, the key cost drivers are the CAPEX in the CO₂ capture cost, CO₂ transport cost, and CO₂ storage cost, which account for about 35, 35, and 15% of the CO₂ avoided cost, respectively. Although the reduction in CO₂ avoided cost by PCC system improvement is apparent, this effect is blunted by the fact

that transport and storage account for ~47–51% of the total cost. Transport cost is non-negligible for coastal countries or countries without onshore storage site in contrast to countries in which relatively cheap onshore pipeline is available (e.g., United States).

Since emissions reduction CCS provides no inherent revenue stream, financial incentives (i.e., carbon price) or regulations are needed. Currently, most of the carbon prices (World Bank, 2020) fall well below (<50 USD/t-CO₂) the CO₂ avoided cost calculated in this study. While the CO₂ price is expected to increase in the coming decades (IEA, 2021), further cost reductions would hasten CCS implementation at the commercial scale. The result in Fig. 9 suggests a promising future direction of research and development in CCS technologies. As mentioned in section 3.1, development of new solutions and processes should take CAPEX reduction, while maintaining low regeneration energies, into consideration. Research and development for facility downsizing or the use of lower cost materials are important levers for the industry. Especially for CO₂ transport and storage, demonstration and implementation are important to reduce the cost through learning-by-doing, scale-out, and market effects.

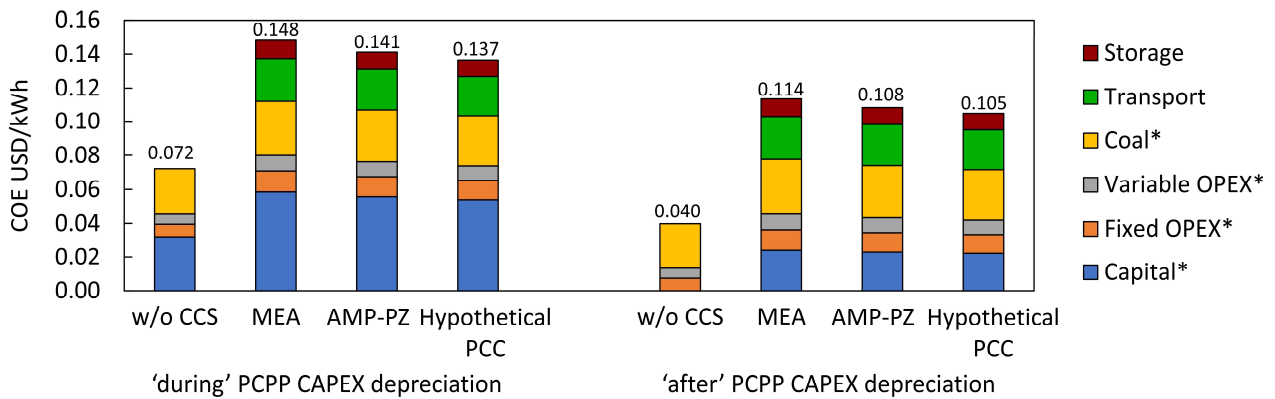


Fig. 8 Breakdown of COE as a function of the PCC system. “*” indicates the breakdown of PCPP-PCC system.

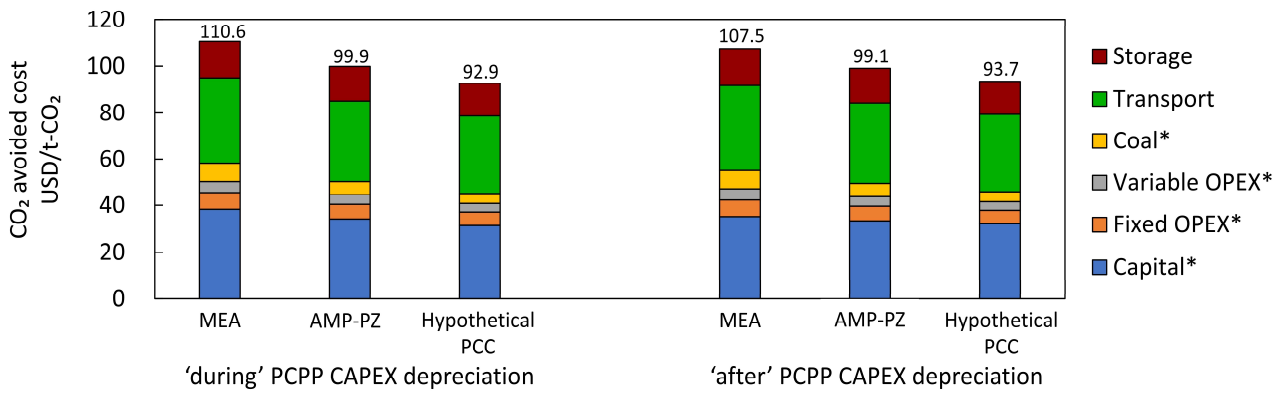


Fig. 9 Breakdown of CO₂ avoided cost as a function of the PCC system. “*” indicates the breakdown of CO₂ capture in the total cost.

4. Conclusions

This study estimated the cost of full chain CCS applied as a retrofit of amine-based CO₂ capture to an existing supercritical pulverized coal thermal power plant in Japan with ship-based transportation, onshore injection into an offshore storage site, and its monitoring. Under the assumed conditions, full chain CCS cost was 99–111 USD/t-CO₂. Switching from the conventional standard solution (i.e., 30wt% monoethanolamine) to the new standard (i.e., the blend of 27wt% 2-amino-2-methyl-1-propanol and 13wt% piperazine) reduced the regeneration energy in the capture process by ~0.85 GJ/t-CO₂, but the full chain CCS cost was only reduced by ~9 USD/t-CO₂. To explore the limits that the PCC performance improvement may have on cost, a hypothetical PCC system with a regeneration energy of ~2.0 GJ/t-CO₂

was modelled; even with this idealized PCC system, the full chain CCS cost was ~93 USD/t-CO₂. This result indicates that switching attention to reducing capital costs (e.g., facility downsizing, cheaper materials of construction) may provide greater returns. Furthermore, since the transportation and storage processes account for ~50% of full chain CCS cost, there is an urgent need to focus research and development on these links in the CCS chain. For countries such as Japan where onshore transport and storage is not a practical option, transport costs are non-negligible. If CCS is going to fulfill the promise by net-zero models and pledges, it is time for it to move from laboratory investigations to real-world implementation. This act of implementation offers the best opportunity for further cost reductions due to the high CAPEX nature of the capture and several transport sub-processes.

Nomenclature

Symbols and constants

a	Reaction order
C	Molar concentration mol/L
CAPEX	Capital expenditure in CO ₂ transport
CF	Capacity factor
COE	Cost of electricity
E	Activation energy kJ/kmol
FCR	Fixed charge rate
K	Chemical equilibrium constant
k^0	kinetic constant kmol/(m ³ ·s) or m ³ /(kmol·s)
MW	Net power output
OC	Operating cost
OPEX	Operating cost in CO ₂ transport
R	Gas constant kJ/(kmol·K)
r	Reaction rate kmol/(m ³ ·s)
T	Temperature K
TASC	Total as-spent capital
TOC	Total overnight cost
ΔG°	Change of Gibbs free energy kJ/kmol

Indices

fix	Fixed
var	Variable
0	Reference

Appendix A.

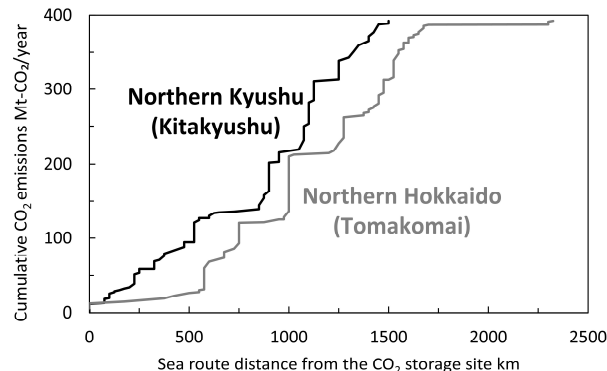


Fig. A1 Cumulative CO₂ emissions from the thermal power plants in Japan as a function of the sea route distance between the emission source and two promising CO₂ storage sites (southern Hokkaido and northern Kyushu).

Acknowledgements

We gratefully acknowledge the assistance of Mr. Kawaharazuka and Ms. Ishihara in the Nakagaki Laboratory.

References

- Abu-Zahra, M. R. M., Niederer, J.P.M., Feron, P.H.M. and Versteeg, G.F., CO₂ capture from power plants Part II. A parametric study of the economical performance based on mono-ethanolamine, International Journal of Greenhouse Gas Control, Vol.1, No.2 (2007), pp.135–142, DOI:10.1016/S1750-5836(07)00032-1.
- Aspen Technology, Rate-based model of the CO₂ capture process by MEA using Aspen Plus (2008a), Burlington, USA.
- Aspen Technology, Rate-based model of the CO₂ capture process by mixed PZ and MDEA using Aspen Plus (2008b), Burlington, USA.
- Aspen Technology, Rate-based model of the CO₂ capture process by AMP using Aspen Plus (2008c), Burlington, USA.
- Baroudi, H. A., Awoyomi, A., Patchigolla, K., Jonnalagadda, K. and Anthony, E.J., A review of large-scale CO₂ shipping and marine emissions management for carbon capture, utilization and storage, Applied Energy, Vol.287, (2021), 116510, DOI:10.1016/j.apenergy.2021.116510.
- Bishnoi, S. and Rochelle, G.T., Absorption of carbon dioxide into aqueous piperazine: Reaction kinetics, mass transfer and solubility, Chemical Engineering Science, Vol. 55, No.22 (2000), pp.5531–5543, DOI:10.1016/S0009-2509(00)00182-2.
- Bishnoi, S. and Rochelle, G.T., Absorption of carbon dioxide in aqueous piperazine/methyldiethanolamine, American Institute of Chemical Engineers Journal, Vol.48, No.12 (2002), pp.2788–2799, DOI:10.1021/ie50367a023.
- Chou, V., Kuehn, N., Lewis, E., Turner, M. and Woods, M., Eliminating the derate of carbon capture retrofits (2016), United States, DOI:10.2172/1510790.
- Edwards, T.J., Maurer, G., Newman, J. and Prausnitz, J.M., Vapor-liquid equilibria in multicomponent aqueous solutions of volatile weak electrolytes, American Institute of Chemical Engineers Journal, Vol.24, No. 6 (1978), pp.966–976, DOI:10.1002/aiic.690240605.
- Element energy, Shipping CO₂ – UK cost estimation study final report for business (2018), Energy & Industrial Strategy Department.
- Energy Information Center, Industrial oil prices, PPS-NET (online), available from <https://pps-net.org/heavy_oil_ac>, (accessed on 13 November, 2021), (in Japanese).
- Ermatchkov, V., Kamps, Á.P. and Maurer, G., Chemical equilibrium constants for the formation of carbamates in (carbon dioxide + piperazine + water) from ¹H-NMR-spectroscopy, Journal of Chemical Thermodynamics, Vol. 35, No.8 (2003), pp.1277–1289, DOI:10.1016/S0021-9614(03)00076-4.
- Feron, P.H.M. Ed., Absorption-based post-combustion capture of carbon dioxide (2016), p. 699, Elsevier Science & Technology.
- Feron, P. H. M., Cousins, A., Jiang, K., Zhai, R. and Garcia, M., An update of the benchmark post-combustion CO₂-capture technology, Fuel, Vol.273, No.1 (2020), 117776. DOI:10.1016/j.fuel.2020.117776.
- GCCSI, Global costs of carbon capture and storage 2017 update (2017).
- GCCSI, Technology readiness and costs of CCS (2021).
- Goto, K., Yogo, K. and Higashii, T., A review of efficiency penalty in a coal-fired power plant with post-combustion CO₂ capture, Applied Energy, Vol.111, (2013), pp.710–720, DOI:10.1016/j.apenergy.2013.05.020.
- Hartono, A., Ahmad R., Usman, M., Asif, N. and Svendsen, H. F., Solubility of CO₂ in 0.1M, 1M and 3M of 2-amino-2-methyl-1-propanol (AMP) from 313 to 393K and model representation using the eNRTL framework, Fluid Phase Equilibria., Vol. 511, No.1 (2020), pp.1–16, DOI:10.1016/j.fluid.2020.112485.
- IEA, World energy outlook 2021 (2021).
- IEAGHG, CO₂ capture at gas fired power plants (2012).
- IEAGHG, The status and challenges of CO₂ shipping infrastructures (2020).
- Intercontinental Exchange, EUA futures | ICE (theice.com) (Online), available from <<https://www.theice.com/products/197/EUA-Futures/data?marketId=5474735&span=3>>, (accessed on 5 December, 2021).
- Isogai, H. and Nakagaki, T., Mechanistic analysis of post-combustion CO₂ capture performance during amine

- degradation, International Journal of Greenhouse Gas Control, Vol.114, (2022), 103597. DOI:10.1016/j.ijggc.2022.103597.
- Japan LP Gas Association, Summary of heating value and CO₂ emission intensity of fuel (online), available from <https://www.j-lpgas.gr.jp/nenten/data/co2_ichiran.pdf>, (accessed on 6 January, 2022), (in Japanese).
- Japan Machinery Center for Trade and Investment, 2012 PCI/LF (Plant Cost Index/Location Factor) report (2012), (in Japanese).
- Japan Machinery Center for Trade and Investment, 2020 PCI/LF (Plant Cost Index/Location Factor) report (2020), (in Japanese).
- Kim, I. and Svendsen, H.F., Comparative study of the heats of absorption of post-combustion CO₂ absorbents, International Journal of Greenhouse Gas Control, Vol.5, No.3 (2011), pp.390–395, DOI:10.1016/j.ijggc.2010.05.003.
- Lucquiaud, M., Steam cycle options for capture-ready power plants, retrofits and flexible operation with post-combustion CO₂ capture, Doctoral thesis at Imperial College London, (2010).
- Ministry of Economy, Trade and Industry, Report of Tomakomai CCS Demonstration Project at 300 thousand tonnes cumulative injection (“Summary Report”) (2020), (in Japanese).
- Ministry of Economy, Trade and Industry, Strategic energy plan | Agency for natural resources and energy (online), available from <https://www.enecho.meti.go.jp/en/category/others/basic_plan/>, (accessed on 2 December, 2021a).
- Ministry of Economy, Trade and Industry, High pressure gas safety act (online), available from <<https://elaws.e-gov.go.jp/document?lawid=326AC0000000204>>, (accessed on 22 December, 2021b), (in Japanese).
- Ministry of the Environment, CCUS's early society implementation conference (3rd) - History and prospects for decarbonization – (3) storage technology (online), available from <<http://www.env.go.jp/earth/ccs/ccus-kaigi/ccus2021.html>>, (accessed on 13 November, 2021a), (in Japanese).
- Ministry of the Environment, Emission factor related page by electric utility (online), available from <<http://www.env.go.jp/press/files/jp/104452.pdf>>, (accessed on 13 November, 2021b), (in Japanese).
- Mitsubishi Heavy Industry, Report on ship transport of CO₂ (2004).
- National Energy Technology Laboratory, FE/NETL CO₂ transport cost model (2018), U.S. Department of Energy, DOI: 10.2172/1556911.
- Oexmann, J. and Kather, A., Minimising the regeneration heat duty of post-combustion CO₂ capture by wet chemical absorption: The misguided focus on low heat of absorption solvents, International Journal of Greenhouse Gas Control, Vol.4, (2010), pp.36–43, DOI:10.1016/j.ijggc.2009.09.010.
- Peters, G.P., Andrew, R.M., Canadell, J.G., Fuss, S., Jackson, R.B., Korsbakken, J.I., Quéré, C.L. and Nakicenovic, N., Key indicators to track current progress and future ambition of the Paris Agreement, Nature Climate Change, Vol.7, (2017), pp.118–122, DOI:10.1038/nclimate3202.
- Posey, M.L. and Rochelle, G.T., A thermodynamic model of methyldiethanolamine-CO₂-H₂S-water, Industrial and Engineering Chemistry Research, Vol.36, No.9 (1997), pp.3944–3953, DOI:10.1021/ie970140q.
- Prime Minister of Japan and His Cabinet, Policy speech by the Prime Minister to the 203rd session of the Diet (Speeches and Statements by the Prime Minister) (online), available from <https://japan.kantei.go.jp/99_suga/statement/202010/_00006.html>, (accessed on 26 December, 2021).
- Psarras, P., He, J., Pilorgé, H., McQueen, N., Jensen-Fellows, A., Kian, K. and Wilcox, J., Cost analysis of carbon capture and sequestration from U.S. natural gas-fired power plants, Environmental Science & Technology, Vol. 54, No. 10 (2020), pp.6272–6280, DOI:10.1021/acs.est.9b06147.
- Rochelle, G., Chen E., Freeman, S., Van Wagener, D., Xu, Q. and Voice, A., Aqueous piperazine as the new standard for CO₂ capture technology, Chemical Engineering Journal, Vol.171, No.3 (2011), pp.725–733, DOI:10.1016/j.cej.2011.02.011.
- Saha, A.K., Bandyopadhyay, S.S. and Biswas, A.K., Kinetics of absorption of CO₂ into aqueous solutions of 2-amino-2-methyl-1-propanol, Chemical Engineering Science, Vol.50, No.22 (1995), pp.3587–3598, DOI:10.1016/0009-2509(95)00187-A.
- Silkenbäumer, D., Rumpf, B. and Lichtenhaler, R.N., Solubility of carbon dioxide in aqueous solutions of 2-amino-2-methyl-1-propanol and N-methyldiethanolamine and their mixtures in the temperature range from 313 to 353 K and pressures up to 2.7 MPa, Industrial and Engineering Chemistry Research Vol.37, No.8 (1998), pp.3133–3141, DOI:10.1021/ie970925w.

TEPCO Energy Partner, Inc., Extra-high voltage power service B (online), available from <https://www.tepco.co.jp/ep/corporate/plan_h/plan08.html>, (accessed on 1 March, 2022), (in Japanese).

Theis, J., Cost estimation methodology for NETL assessments of power plant performance (2019), United States, DOI:10.2172/1567185.

Tong, D., Trusler, J.P.M., Maitland, G.C., Gibbins, J. and Fennell, P.S., Solubility of carbon dioxide in aqueous solution of monoethanolamine or 2-amino-2-methyl-1-propanol: Experimental measurements and modelling, International Journal of Greenhouse Gas Control, Vol.6, (2012), pp.37–47, DOI:10.1016/j.ijggc.2011.11.005.

Trade Statistics of Japan, Statistical table, Article: COAL N.E.S., General code: 2701.12-099 (online), available from <<https://www.customs.go.jp/toukei/srch/index.htm?M=29&P=1,2,,,,,,4,1,2020,0,0,0,2,270112099,,,,,,,,,,,20,>>, (accessed on 15 June, 2021).

Tribe, M. A. and Alpine, R. L. W., Scale economies and the "0.6 rule", *Engineering Costs and Production Economics*, Vol. 10, No. 1 (1986), pp.271-278, DOI:10.1016/0167-188X(86)90053-4.

Van Wagener, D.H., Stripper modeling for CO₂ removal using monoethanolamine and piperazine solvents, Doctoral thesis at Technical University of Texas at Austin, (2011).

Wang, N., Akimoto, K. and Nemet, G.F. What went wrong? Learning from three decades of carbon capture, utilization and sequestration (CCUS) pilot and demonstration projects, Energy Policy, Vol. 158, (2021), 112546, DOI:10.1016/j.enpol.2021.112546.

World Bank, State and trends of carbon pricing 2020 (2020), World Bank, Washington, DC, DOI: 10.1596/978-1-4648-1586-7.

Zoelle, A., Keairns, D., Turner, M., Woods, M., Kuehn, N., Shah, V., Chou, V. and Pinkerton, L., Cost and performance baseline for fossil energy plants volume 1a: bituminous coal (PC) and natural gas to electricity revision 3 (2015), United States, DOI:10.2172/1480987.